

## Supplemental Material for Jiang *et al*,

### Tumor Imaging via Proteolytic Activation of Cell Penetrating Peptides

#### Reagents

Fmoc protected amino acids and synthesis resins were purchased from EMD Chemicals Inc. Dimethylformamide (DMF), piperidine, and 2-(1H-9-azabenzotriazole-1-yl)-1,1,3,3-tetramethyluronium hexafluorophosphate (HATU) were from Applied Biosystems. Trifluoroacetic acid (TFA), thioanisole, triisopropylsilane, ethanedithiol, and diisopropylethylamine (DIEA) were from Sigma-Aldrich. 5(6)-Carboxyfluorescein succinimidyl ester and 5-iodoacetamidofluorescein were from Molecular Probes. Cy5 monoreactive NHS ester and Cy5 monomaleimide were from Amersham Biosciences. MMP-2 proenzyme and MMP-9 were from EMD. Enterokinase and urokinase plasminogen activator (uPA) were from Invitrogen and Alexis, respectively. Methoxy PEG-maleimide (5 KDa, 21 KDa) was purchased from Nektar and methoxy PEG-maleimide (11 KDa) was supplied by SunBio PEG-SHOP, Korea. All reagents were used as obtained without further purification.

#### Peptide Synthesis and Fluorophore Labeling

Peptides were synthesized on an automatic peptide synthesizer (Pioneer Peptide Synthesis System by Applied Biosystems) using standard protocols for Fmoc solid phase synthesis. After the peptide was synthesized, the resin was washed with dimethylformamide, dichloromethane, and methanol 3 times each and vacuum dried for 3 hr. The peptides were cleaved off the resin overnight with either  $\text{CF}_3\text{COOH}$  /thioanisole/triisopropylsilane (96/2/2, v/v) for peptides without a sulfhydryl group, or

CF<sub>3</sub>COOH/thioanisole/triisopropylsilane/ethanedithiol (94/2/2/2, v/v) for peptides with a sulfhydryl group. The cleavage solution was evaporated nearly to dryness, and the crude peptide was triturated with ether and vacuum dried for 3 hr. Fluorophores were attached to peptides either before or after cleavage from the resin; 5(6)-carboxyfluorescein *N*-hydroxysuccinimidyl ester and Cy5 monoreactive *N*-hydroxysuccinimidyl ester labeled amino groups, whereas 5-iodoacetamidofluorescein and Cy5 monomaleimide reacted with sulfhydryl groups. Finally, fluorophore labeled peptides were purified on HPLC (C<sub>18</sub> reverse phase column, eluted with 10-40% acetonitrile in water with 0.1% CF<sub>3</sub>COOH) and lyophilized overnight. The molecular weight of all peptides was confirmed by mass spectroscopy, and the concentration of each peptide stock solution was verified by UV-vis absorbance.

### **Peptide disulfide bond formation and reduction**

Peptides with cysteine residues were cleaved off the resin via standard procedures. To form a cyclic disulfide, vacuum dried crude peptide was diluted to 1 mg/ml in 5 mM NH<sub>4</sub>HCO<sub>3</sub> and vigorously stirred in air for 3 hr. The crude cyclic peptide was purified on HPLC (C<sub>18</sub> reverse phase column, eluted with 10-40% acetonitrile in water with 0.1% TFA) and lyophilized overnight. As before, the molecular weight of each peptide was confirmed by mass spectroscopy, and the concentration of the stock solution was verified by UV-vis absorbance. To obtain the linear peptide, the disulfide bond was reduced by mixing equal volumes of 100 μM cyclic peptide, 10 mM TCEP [tris(2-carboxyethyl)phosphine], and 100 mM MES [2-mercaptoethanesulfonic acid, sodium salt] in PBS and incubating at room temperature for 30 min. Reduction was

confirmed by HPLC and mass spectroscopy. The final concentrations of TCEP and MES in the media during cell uptake assays were 0.5 and 5 mM respectively.

### **PEGylated peptide synthesis and Cy5 labeling**

Peptides with free thiol groups at the N-terminus were synthesized using a standard Fmoc peptide synthesis protocol, except that the final amino acid coupled to the resin was tritylmercaptoacetic acid. The peptide was cleaved off the resin through the standard procedure described earlier and reacted with 0.5 –0.8 equivalent methoxy PEG-maleimide in DMF and 100-fold excess 4-methylmorpholine as base at room temperature for over 12 hours. Solvent and excess base were evaporated off under vacuum. The pegylated peptide was labeled with Cy5 by reacting with 2-3 equivalent Cy5 mono NHS ester in 50 mM sodium bicarbonate solution at room temperature overnight. The crude product was purified on HPLC and then lyophilized.

### **ACPP Cleavage by Enterokinase**

10  $\mu$ l of a 0.38 mM peptide stock solution dissolved in water was mixed with 10  $\mu$ l 1 U/ $\mu$ l enterokinase (Invitrogen) and incubated at 37°C. Enzymatic cleavage was monitored by injecting 5  $\mu$ l of the reaction mixture on HPLC and observing either UV-vis absorbance at 440 nm for fluorescein labeled or 650 nm for Cy5 labeled peptide. The HPLC chromatograms showed that cleavage by enterokinase was nearly complete after 15 min incubation time. The new peaks were collected and their identities were determined by mass spectroscopy. The mass spectra indicated that the enzyme cut between lysine and alanine residues of the enterokinase substrates as expected.

### **ACPP cleaved by urokinase plasminogen activator (uPA)**

100  $\mu$ M peptide in 400  $\mu$ l PBS (Phosphate Buffered Saline, pH7.4) was incubated at 37°C with 6  $\mu$ g uPA for over 3 hours. The cleavage progress was monitored on HPLC. Mass spectroscopy on HPLC fractions indicated that the cleavage was close to completion after 3 hr and that the enzyme cleavage site was between arginine and serine residues in the peptide as expected (1) (MS: 2688.6 found, 2688.2 calculated).

### **Conformational analysis by two-dimensional NMR**

We have studied the peptide using homonuclear two-dimensional NMR spectra in order to assess structural proclivities of the native ensemble. The NMR samples were prepared in 90% H<sub>2</sub>O, 10% D<sub>2</sub>O buffer containing 50 mM potassium phosphate, pH 6.5. Peptide concentration was 2.69 mM and spectra were recorded at 5 °C. NMR spectra were collected using a Bruker DMX 500 MHz spectrometer and a Varian UnityPlus 800 MHz spectrometer. DQF-COSY, TOCSY, and NOESY spectra were collected using standard pulse sequences (see (2) and references therein). All spectra were collected using the 3-9-19 pulse sequence with gradients for water suppression (3). The NOE mixing time was 500 ms and the TOCSY mixing time was 60 ms.

Spectral processing was performed using Felix (Molecular Simulations Inc., San Diego, CA). Apodizations in the t<sub>2</sub> and t<sub>1</sub> dimensions were with cosine squared window functions and the solvent was deconvoluted from the spectra using the time domain convolution method (4) with a sine bell function.

As expected, there is chemical shift degeneracy and spectral overlap introduced by the strings of D-glu and D-arg residues (DQF-COSY data not shown). We can classify the resonances of the D-glu and D-arg residues by type and make sequence-specific assignments of the resonances of linker region, i.e. XPLGLAG. In Figures 6 and

7, the consistency of the observed NOEs are assessed relative to the sequential and medium-range NOEs expected for a  $\beta$ -turn and the long-range NOES for cross-strand interactions.

Figure 6A shows the  $H^\beta/H^\gamma$ /sidechain ( $\delta_1$ )- $H^N$ ( $\delta_2$ ) region of the NOESY spectrum, and Figure 6B shows the identical region for the TOCSY spectrum. The  $H^\beta$  and  $H^\gamma$  shifts of the D-glu and D-arg resonances are labeled in the TOCSY. Significant chemical shift overlap is present among  $H^\beta$  and  $H^\gamma$  resonances, but resonances by amino acid types are well resolved. In both Figure 6A and 6B, there is a cluster of  $H^\beta$  and  $H^\gamma$  shifts at 1.7/1.78 and 1.55/1.66 respectively for D-arg and  $H^\beta$  and  $H^\gamma$  shifts at 1.95/2.03 and 2.25/2.3 respectively for D-glu. In the NOESY spectrum (Fig. 6A), we see evidence for cross-strand interactions between the string of D-arg and the string of D-glu.residues. NOE cross-peaks at 1.92, 2.03, 2.25, and 2.29 ( $\delta_1$ ) and 8.65 ( $\delta_2$ ) are consistent with through space interactions between the  $H^\beta$  and  $H^\gamma$  sidechain of one or more D-glu and the  $H^N$  backbone of one or more D-arg.

For clarity, 1D vectors drawn from selected D-arg and D-glu backbone  $H^N$  resonances ( $\delta_2$ ) (see dashed blue lines in Figure 6A and 6B) are depicted in Fig. 6C –6E. Fig. 6C is drawn from the NOESY spectrum at 8.65 ppm ( $\delta_2$ ), the  $H^N$  resonance of a D-arg, with  $H^\beta$  and  $H^\gamma$  signals of both D-glu and D-arg present. Fig. 6D is drawn from the TOCSY spectrum at the same  $\delta_2$  shift and  $H^N$  resonance, with only the  $H^\beta$  and  $H^\gamma$  signals of D-arg. Fig. 6E is also drawn from the TOCSY spectrum but 8.59 ppm ( $\delta_2$ ), the  $H^N$  resonance of a D-glu, with only the  $H^\beta$  and  $H^\gamma$  signals of D-glu.

Fig. 7 shows the  $H^N$  ( $\delta_1$ )- $H^N$ ( $\delta_2$ ) region of the NOESY spectrum. There are five cross-peaks labeled with sequence-specific identification, indicating sequential  $H^N$ - $H^N$

backbone interactions among the residues of the linker region and the neighboring D-glu and D-arg on either side. This type of short-range NOE is consistent with turn or helical secondary structure (5).

### **Potential interactions with furin**

Up to now, we have relied almost exclusively on 9 arginines, usually D-, in a row, partly for simplicity and partly because they are amongst the most effective uptake sequences (6, 7). However, very recently nona-D-arginine amide has been reported to be a potent inhibitor of furin, a well-known processing protease (8). Given the highly electrostatic nature of the binding, it is quite likely that the intact substrate with polyanionic domain still attached will be a much poorer inhibitor of furin. If this prediction is verified experimentally, then the furin inhibition may be unimportant or beneficial, because it will be mainly in target tissue such as tumors that furin is acutely inhibited.

### **Imaging of SCCA samples with ACPP's following administration of an MMP inhibitor**

Since MMP's are dependent on zinc for activation, we used the lipid soluble, high affinity  $Zn^{2+}$  chelator TPEN (*N,N,N',N'*-tetrakis-(2-pyridylmethyl)ethylenediamine) (9) as a broad spectrum MMP inhibitor to preliminarily assess whether cleavage and retention of our peptide in SCCA tumors was MMP dependent. Fresh SCCA slices were incubated in HBSS (Fig. 8A) or 1  $\mu$ M TPEN in HBSS (Fig. 8B) at room temperature for 15 minutes. Slices were then stained with 1  $\mu$ M cleavable peptide alone (Fig. 8A) or 1  $\mu$ M cleavable peptide plus 1  $\mu$ M TPEN (Fig. 8B) before being washed five times in fresh

HBSS and cryosectioned. The images shown below were taken using a 10x objective, and hematoxylin/eosin staining was used to verify tissue type.

Fig. 6

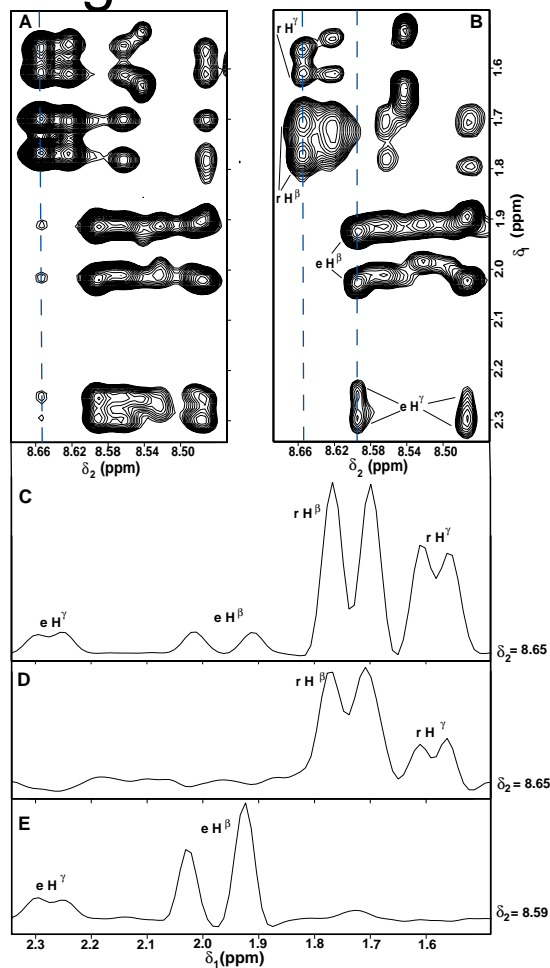


Figure 6. NMR spectra of the  $H^{\beta/\gamma}(\delta_1)$ - $H^N(\delta_2)$  region of the peptide. Evidence for cross-strand interactions between D-arg and D-glu residues. **A.** NOESY spectrum. Blue dashed line at 8.65 ppm corresponds to C. **B.** TOCSY spectrum. Blue dashed lines at 8.65 and 8.59 correspond to D and E, respectively. **C.** 1D NOESY vector at the  $H^N$  of a D-arg. **D.** 1D TOCSY vector at the  $H^N$  of a D-arg. **E.** 1D TOCSY vector at the  $H^N$  of a D-glu.

Fig. 7

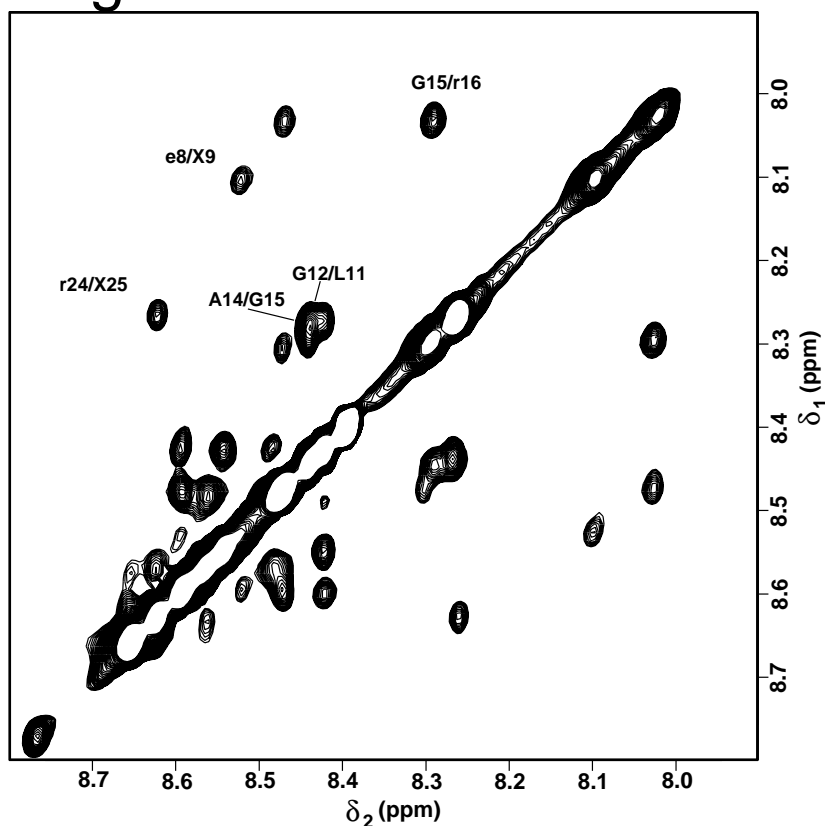


Figure 7. NOESY spectrum of the  $H^N(\delta_1)$ - $H^N(\delta_2)$  region indicates sequential  $H^N$ - $H^N$  backbone interactions through the residues of the linker region. Symmetry related cross-peaks are labeled once at either side of the diagonal.

**Fig. 8**

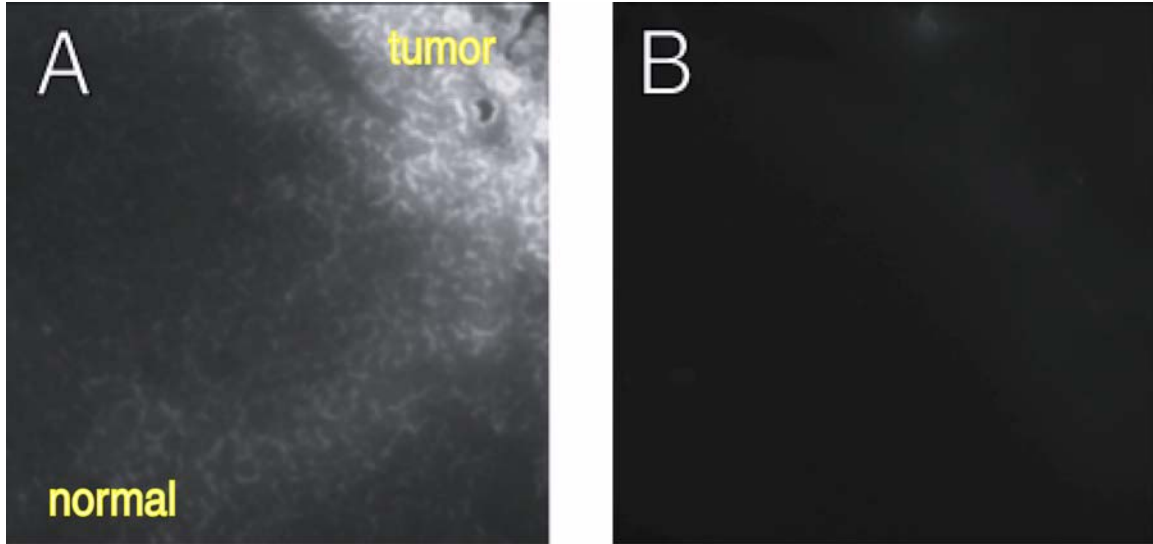


Fig. 8. TPEN inhibits staining of squamous cell carcinoma specimens by a cleavable ACPP, (5 kDa PEG)-eeeeeeeeeXPLGLAG-rrrrrrrrrXk(Cy5), where X denotes 6-aminohexanoyl. Tissue slices were stained with 1  $\mu$ M ACPP in the absence (A) or presence (B) of 1  $\mu$ M TPEN. The slice shown in (A) contains regions of tumor (top right) as well as normal tissue. The slice shown in (B) contains only tumor.

## Reference List

1. Ke, S. H., Coombs, G. S., Tachias, K., Corey, D. R. & Madison, E. L. (1997) *J. Biol. Chem.* **272**, 20456-20462.
2. Ernst, R. R., Bodenhausen, G. & Wokaun, A. (1990) *Principles of Nuclear Magnetic Resonance in One and Two Dimensions* (Oxford University Press, Oxford).
3. Piotto, M., Saudek, V. & Sklenar, V. (1992) *J. Biomol. NMR* **2**, 661-665.
4. Marion, D., Ikura, M. & Bax, A. (2004) *J. Magn. Reson.* **84**, 425-430.
5. Wüthrich, K. (1986) *NMR of Proteins and Nucleic Acids* (John Wiley & Sons, New York).
6. Mitchell, D. J., Kim, D. T., Steinman, L., Fathman, C. G. & Rothbard, J. B. (2000) *J. Peptide Res.* **56**, 318-325.
7. Gammon, S. T., Villalobos, V. M., Prior, J. L., Sharma, V. & Piwnicka-Worms, D. (2003) *Bioconjugate Chem.* **14**, 368-376.
8. Kacprzak, M. M., Peinado, J. R., Than, M. E., Appel, J., Henrich, S., Lipkind, G., Houghten, R. A., Bode, W. & Lindberg, I. (2004) *J. Biol. Chem.* **279**, 36788-36794.
9. Arslan, P., Di Virgilio, F., Beltrame, M., Tsien, R. Y. & Pozzan, T. (1985) *J. Biol. Chem.* **260**, 2719-2727.